Analysis of the Results of the Study of the Thermoelectric Part of the Source Sensor

Mamadalieva Lola Kamiljanovna
Doctor of Technical Sciences, Docent, Fergana polytechnic institute, Uzbekistan

Minamatov Yusupali Esonali ugli
Assistant, Fergana polytechnic institute, Uzbekistan

ABSTRACT

The article discusses the features of the thermoelectric part of the sensor - the source, which is included in this design, gives more electrical power at the output with a large temperature difference and a good value of the parameter Z.

KEYWORDS: *thermoelement, source sensor, temperature dependence, hot and cold thermoelement junctions, films, n-type, selenium, tellurium, stibium, quartz, efficiency, thermoelement, extremum, electron, Peltier and Thomson effect.*

Introduction. According to the results of numerous studies of thermoelements, thermopiles and thermoelectric materials [1-9] show that the main factors influencing the efficiency are: the temperature difference between cold and hot junctions of FC and the figure of merit of materials Z.

The temperature dependences of the electrophysical parameters have been studied quite well. Hence, a strong, and sometimes noticeably complex, dependence of these parameters on temperature was established. The temperature itself, in the case under consideration, is a function of the density of the incident radiation. In addition, the presence of the photoconverting part of the source sensor is considered to be an influencing factor on the temperature value supplied to the hot junctions of the TB. This is due to the following: although the supply energy is not completely converted into electrical energy by the photosensitive film, part of the energy corresponds to the formation of anomalous photovoltage at the output of the converter. The next important factor is the reflection from the front surface of the transducer. If we deeply analyze the well-known law of conservation of energy, then it becomes obvious that light radiation with a spectrum with different wavelengths of light is not uniformly converted into heat. "White" light and ultraviolet radiation, in comparison with infrared radiation, gives little heat, and this part of the radiation remains practically useless for the thermal converter. This task is apparently successfully solved by creating such combined devices as recommended by us.

The study, verification and analysis of the results of the assigned task shows the reliability of the proposed conclusions.

Figure 1 shows the dependence of the temperature of the hot junction of the thermoelement on the value of the incident light energy on the light-receiving surface.

As can be seen from the figure, this characteristic has a linear character, that is, the temperature of the hot junction of thermopiles, although implicitly, but linearly depends on the integrated power of the supplied light energy. Straight line 1 corresponds to a temperature of + 200C of the cold junction of thermopiles.

A decrease in the temperature of the cold end of the thermopile helps to reduce the temperature of the hot junction, due to additional heat removal from T_g. To reach the hottest temperature on the hot junction of the thermopile, the light-sensing surfaces of the TB should be illuminated with the most powerful light intensity (or the surface of a photosensitive structure of the film type). Under laboratory conditions, this problem is solved by increasing the value of the filament current of the lamp simulating light radiation - tungsten incandescent lamps or the value of the operating current of lamps of arc-discharge design and brand. Thus, straight line 2 in Figure 2. corresponds to a temperature of -20^{0}C and 3-60^{0}C at the given values of the density of the supplied light energy.

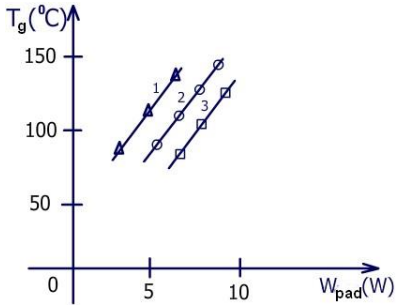

Fig. 1. Dependency *f* (W_{pad}) 1,2,3

T_g – respectively: +20^{0}C-1; -20^{0}C-2; -60^{0}C-3.

As for the spectral distribution of light by wavelength, it was found that this parameter is different for different simulators of light radiation. The closest, in this sense, to solar radiation is radiation from ultra-high-pressure arc-discharge lamps, that is, xenon.

Temporarily putting aside the spectral dependence of the temperature T_g of the junction, let us consider the dependences of the maximum power of the efficiency of the thermopile on the heat flux entering the hot junctions.

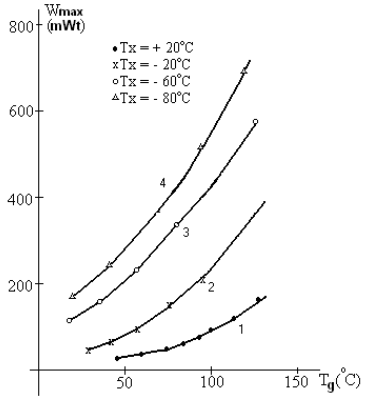

Fig. 2. Dependence of the maximum power of the thermopile from hot junction temperature T_g.

Figure 3 shows the dependence of the useful power generated at the thermopile load on T_g. It can be seen that with an increase in temperature at the beginning this parameter grows linearly, then it has an over-linear dependence. The reason for this is, as shown in [1], the positive effect of the phonon part of the conductivity.

Efficiency d. battery grows sublinearly with increasing temperature (Fig. 3.). This can be explained, probably, by the optimal operating temperatures of thermoelectric materials, the effect of temperature on the values of electrophysical parameters, and, of course, on the thermoelectric figure of merit Z.

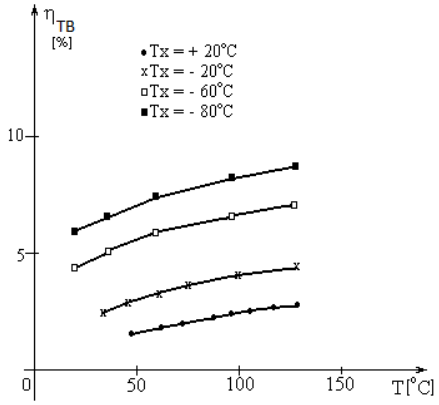

Fig. 3. Dependencies of efficiency thermopile from hot junction temperature at different cold junction temperatures.

An important stage in the study of the thermoelectric part of the design being developed is to take into account and determine the geometric dimensions of the optimal design. This is explained by the following: the value of the operating current is a function of the cross-section and the length of the thermoelement legs. Changing the size of thermopiles affects not only the electrophysical parameters of the device, but also their economic indicators.

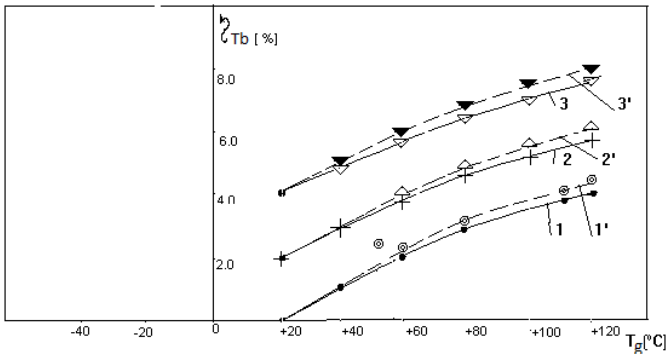

Fig.4. Dependencies of efficiency thermopile from the hot junction temperature at

values Tx=+20°C (1,1′), - 20°C (2,2′) и - 60°C (3,3′).

Calculated and experimental values of the efficiency dependence TB versus T_g are shown in Fig. 4. It can be seen here that with an increase in $\Delta T=T_g+T_x$, the efficiency increases. batteries and, the lower Tx, the higher η_{tb}; Here, the dashed lines show the calculated values and the solid lines show the experimental values.

Efficiency d. battery is found by the formula:

$$\eta_{Tb} = W_{max}/(Q_P+Q_\chi) \qquad (1)$$

Formula (1.) differs from Ioffe's formula in that the formula was obtained under the assumption that α, χ, ρ, as well as Z branches do not depend on temperature closer to the truth, since here the discrepancy σ (ρ) is taken into account (i.e., the mean integral value ρ is taken, and not $\alpha^2 \sigma / \chi = Z$). The temperature dependence of all Z components leads to a decrease in the real efficiency. in comparison with the calculated according to (2.). This is explained by a sharp decrease in Z = Z (T) with increasing temperature after passing the maximum, which is mainly due to the onset of intrinsic conductivity and the bipolar mechanism of thermal conductivity, as well as the electrical mismatch of individual sections of the legs, associated with the temperature gradient along the length of the

legs and the temperature dependence of the electrical resistance of the material. Efficiency values thermopiles calculated by the formula which, although it is approximate, but better takes into account the temperature dependences of the characteristics of the material (α, χ, ρ,), usually agree well with the experimentally measured ones.

For comparison with Ioffe's formula:

$$\eta_{max} = \frac{T_g - Tx}{T_g} \cdot \frac{M_0 - 1}{M + \frac{Tx}{T_g}} \qquad (2)$$

we transform (1.) into the form:

$$max = \frac{\Delta T}{T_g} \cdot \frac{\xi_{T\text{э}}}{\xi} \cdot \frac{M_0 + C}{M_0 + A} \cdot \frac{M_0 - \frac{1+A}{1+P}}{M_0 + A\frac{1+P}{2}\cdot\frac{Tx}{T_g} + \left(A\frac{1+P}{2} - \frac{1+A}{1+P}\right) + \frac{(1+P)A - \frac{(1+A)^2}{1+P}}{Z_{T\text{э}} T_g}} \qquad (3)$$

where,

$$P = \frac{B - \frac{D}{A}}{1 + Z_{T_\text{э}} T' cp}.$$

This expression can be written as the product of three efficiency factors. First, the efficiency. Karnot $\eta_k = \Delta T/T_g$, allowing to calculate the efficiency. ideal reversible cycle of a heat engine operating in the temperature range (T_g, T_x). External irreversibility, i.e. the fact that the thermoelement operates not at a temperature difference $\Delta T = T_g - T_x$, but at $\Delta T < \Delta T'$, allows one to take into account the efficiency. heat pipe $\eta_{т} = \xi_{Tэ}/\xi$. The lagging part of expression (3), which we call thermoelectric efficiency $\eta_{TЭ}$, allows to take into account the irreversible losses associated with thermal conductivity through the thermoelement and the irreversible release of Joule heat in it.

Table 1. Results of experimental measurements of TB

l =0,7см, S=0,16мм^2

Tx÷Tg (°C)	E (mW)	r (mOm)	I_{opt} (A)	Q_p (Wt)	Q_T (Wt)	Q (Wt)	Wel (Wt)	η (%)	Wsv (Wt)
20÷120	392	108,325	1,518	2,386	5,22	7,61	0,346	4,547	8,95
-20÷120	536	103,2	2,18	3,426	7,37	10,796	0,678	6,28	12,7
-60÷120	654	94,465	2,93	4,6	9,68	14,28	1,104	7,73	16,8
-80÷120	700	90,5	3,288	5,17	10,91	16,07	1,322	8,23	18,91

Tx÷Tg (°C)	$\rho_n \cdot 10^3$ (Om cm)	α_n (μV / deg)	$\chi_n \cdot 10^3$ (Wt/cm·deg)	$\rho_\rho \cdot 10^3$ (Om cm)	α_ρ (μV / deg)	$\chi_\rho \cdot 10^3$ (Wt/cm·deg)
20÷120	1,266	229,2	15,58	1,538	244,7	14,77
-20÷120	1,176	224	15,99	1,375	236,3	15,04
-60÷120	1,088	217	16,52	1,23	225,5	15,59
-80÷120	1,044	213	16,87	1,162	219,3	15,96

l =1,4см, S=0,16 мм^2

Tx÷Tg (°C)	E (mV)	r (mOm)	I_{opt} (A)	Q_p (Wt)	Q_T (Wt)	Q (Wt)	Wel (Wt)	η (%)	Wsv (Wt)
20÷120	392	216,65	0,759	1,193	2,61	3,805	0,173	4,547	4,475
20÷140	472	232,33	0,853	1,398	3,195	4,595	0,234	5,092	5,405
-20÷120	536	206,43	1,09	1,713	3,685	5,398	0,339	6,28	6,35
-60÷120	654	188,93	1,464	2,3	4,84	7,14	0,552	7,73	8,4

-80÷120	700	181	1,644	2,58	5,455	8,035	0,661	8,227	9,455

Tx÷Tg (°C)	$\rho_n \cdot 10^3$ (Om cm)	α_n (μV / deg)	$\chi_n \cdot 10^3$ (Wt/cm·deg)	$\rho_\rho \cdot 10^3$ (Om cm)	α_ρ (μV / deg)	$\chi_\rho \cdot 10^3$ (Wt/cm·deg)
20÷120	1,745	249,1	13,38	1,583	240,8	15,14
20÷140	1,682	248,9	13,59	1,637	242,3	15,54
-20÷120	1,52	244,78	13,58	1,429	234,21	15,19
-60÷120	1,403	238,7	13,91	1,296	215,77	15,49
-80÷120	1,349	235,0	14,12	1,234	212,4	15,7

Table 1 shows the results of calculating thermoelement legs and its main parameters depending on their length. The above reasoning is clearly demonstrated here. Such studies are also necessary to establish the weight and size characteristics of all types of structures being created.

The experimental values of the electrical and thermal characteristics of the FC legs for different two lengths (l = 0.7 cm, l = 1.4 cm) are given in Table 1. It can be seen from the table that the length of the legs in this case is equal to the efficiency value. practically does not affect. E.m.s. also remains at the same level. The value of the internal resistance of FC branches is growing. The current is almost halved. Heat fluxes are also proportionally reduced due to the Peltier and Thomson effects. Of course, all these phenomena are associated with a proportional decrease in the value of the density of the light incident on the heat-sensing surface of the thermopile.

Conclusions. In conclusion, we can say that, similar to the previous works of researchers, the thermoelectric part of the sensor-source included in this design gives more electrical power at the output with a large temperature difference and a good value of the parameter Z ($3.0 \cdot 10^{-3}$ deg^{-1}).

An analysis of the spectral characteristics of optical radiation as a result of interaction with matter and an analysis of transport phenomena using the thermodynamics of irreversible processes shows that the phenomena of momentum, heat and charge transfer in a gas are essential for understanding what is happening in these processes. Determination of the competitiveness of sensors for monitoring a gas environment largely depends on the research carried out taking into account real conditions.

References:

1. A.M. Kasimaxunova, Maxsudjon Norbutaev, and Madinaxon Baratova. Thermoelectric generator for rural conditions. Scientific progress, vol. 2, no. 6, 2021, pp. 302-308.
2. A.A Xolmatov, J.X Karimov, A.M Xayitov. Effect of crystallizer catalyst on properties of glass-crystalline materials. // EPRA International Journal of Research and Development (IJRD). 2021, pp.273-275.
3. Abduqaxxorovich O. S. et al. Development and research of heterostructures with an internal thin layer based on p-type silicon //European science review. – 2018. – №. 9-10-1.
4. Axmadaliyevich K. A. et al. Possibilities of getting electricity with the help of a small solar furnace //EPRA International Journal of Research & Development. – 2021. – T. 6. – №. 6. – C. 147-151.
5. Kasimakhunova A. M. et al. Photo Thermal Generator of Selective Radiation Structural and Energetic Features //Journal of Applied Mathematics and Physics. – 2019. – T. 7. – №. 06. – C. 1263.
6. Kasimakhunova A. M. et al. Research of AHV-effect in films and crystals with the effect of the double luxurification //Computational nanotechnology. – 2018. – №. 3. – C. 44-48.
7. Kuchkarov A. A., Muminov S. A., Abdurakhmanov A. A. Combined Energy Supply for Sixty-Two Heliostats of the Big Solar Furnace //Journal of Siberian Federal University. Engineering & Technologies. – 2020. – T. 13. – №. 4. – C. 449-454.

8. Mamadalieva L. K. Development of photothermoelectric converters and research of their design and operational features //Euroasian Journal of Semiconductors Science and Engineering. – 2019. – Т. 1. – №. 6. – С. 3.
9. Mamadilieva L. K., Zokirov S. I. Automation problems of finding the optimal coordinates of a photocell in a selective radiation photothermogenerator. – 2019.
10. Muhammad-Sultanhan, Paizullahanov, Sobirov Muslimjon Mukhsinjonugli, Xolmatov Abdurashid Abdurakhimugli. "Materials processing in the solar furnace." ACADEMICIA: An International Multidisciplinary Research Journal. 10.10 (2020): 1233-1237.
11. Muhammad-Sultanhan, Paizullahanov, Sobirov Muslimjon Mukhsinjonugli, Xolmatov Abdurashid Abdurakhimugli. "Materials processing in the solar furnace." ACADEMICIA: An International Multidisciplinary Research Journal. 10.10 (2020): 1233-1237.
12. Okhunov, M., & Minamatov, Y. (2021). Application of Innovative Projects in Information Systems. European Journal of Life Safety and Stability (2660-9630), 11, 167-168.
13. Paizullakhanov MS, Kholmatov AA, Sobirov MM, Khamdamov B. Wear-Resistant Materials Synthesized in A Solar Furnace. // Journal of Material Sciences & Manufacturing Research. 2020.
14. Paizullakhanov MS, Kholmatov AA, Sobirov MM, Khamdamov B. Wear-Resistant Materials Synthesized in A Solar Furnace. // Journal of Material Sciences & Manufacturing Research. 2020.
15. Payzullakhanov Mukhammad-Sultan Saidvalikhanovich, Xolmatov Abdurashid Abdurakhim ugli, Sobirov Muslim Muhsinjon ugli. Magnetic materials synthesized in the sun furnace // International Journal of Advanced Research in Science, Engineering and Technology. 2020. Vol. 7, Issue 4, pp.1499-13505.
16. Каримов Ж. Х., Фозилов И. Р. Управление многостадийными процессами путём оптимизации глобальных целей системы //Universum: технические науки. – 2020. – №. 3-1 (72). – С. 16-20.
17. Касимахунова А. М. и др. Исследования некоторых явлений в АФН-структурах с изовалентными примесями для разработки приборов и устройств неразрушающего контроля и измерения //Computational nanotechnology. – 2018. – №. 2.
18. Кучкаров А. А., Муминов Ш. А. У. Моделирование и создание плоского френелевского линейного зеркального солнечного концентратора //Universum: технические науки. – 2020. – №. 3-2 (72). – С. 80-85.
19. Мамадалиева Л. К. Анализ и выбор монохроматоров для фототермогенератора селективного излучения //Universum: технические науки. – 2020. – №. 6-1 (75). – С. 74-77.
20. Мамадалиева Л. К. и др. Энергосберегающий частотноуправляемый асинхронный электропривод с вентиляторной нагрузкой //Вестник науки и образования. – 2019. – №. 13-2 (67).
21. Мамадалиева Л. К., Набиев М. Б., Усмонов Я. Легирование термоэлектрических материалов на основе Bi2Te3-Sb2Te3 для фототермопреобразователей солнечного излучения //Янги материаллар ва гелиотехнологиялар. – 2030. – С. 90.
22. Пайзуллаханов Мухаммаде-Султанхан Саидивалиханович, Холматов Абдурашид Абдурахим Угли, Собиров Муслимбек Мухсинжон Угли Титанаты бария и стронция, синтезированные на солнечной печи // Universum: технические науки. 2020. №6-1 (75).
23. Холматов А. А. У., Хайитов А. М. Ў. ИЗУЧИТЬ И ИЗУЧИТЬ СВОЙСТВА БАРИЯ И СТРОНЦИЯ-ТИТАНА, СИНТЕЗИРОВАННЫХ В БОЛЬШОЙ СОЛНЕЧНОЙ ПЕЧИ //Oriental renaissance: Innovative, educational, natural and social sciences. – 2021. – Т. 1. – №. 11. – С. 79-93.